Turk Neurosurg, 2024

Original Investigation

DOI: 10.5137/1019-5149.JTN.45091-23.2

Received: 06.08.2023
Accepted: 08.01.2024

Published Online: 25.07.2024

Redefining Diagnostic Criteria for Basilar Invagination Using Linear Craniometric Parameters

Vikrant YADAV, Nityanand PANDEY, Anurag SAHU, Ravi Shankar PRASAD

Institute of Medical Sciences, Banaras Hindu University, Varanasi, Uttar Pradesh, India

Corresponding author: Vikrant YADAV ✉ vikrantyadav473@gmail.com

ABSTRACT

AIM: To establish the diagnosis of basilar invagination (BI) on the basis of specific bony landmarks Klaus' index (KI), perpendicular distance between the tip of the odontoid process and palato internal occipital protuberance (PI) line.

MATERIAL and METHODS: Forty-nine patients were analysed, who underwent surgery for BI, between July 2020 and June 2023. Radiological assessment was done in all the patients using reconstructed midsagittal images on computed tomography scans .

RESULTS: Mean age was 34.82 ± 10.52 years with male preponderance (67.35%) in patients with BI. We also analysed randomly selected 120 control subjects (male: female = 59:61) with mean age 43.5 ± 14.08 years. The mean distance of tip of the odontoid process from PI line in patients with BI was 3.39 ± 3.09 mm. The mean value of KI in the patients with BI was 28.57 ± 1.68 mm. Receiver operating characteristic (ROC)curve was used for analysing the distance of the tip of the odontoid process from PI line in the patients with BI which produced area under curve(AUC) of 0.97 (confidence interval [CI] -0.931 to 0.990, p<0.0001). Cut-off point of 7.5 mm was identified for the distance of tip of odontoid process from PI line with sensitivity of 89.8% and specificity of 97.5% having 95.27% diagnostic accuracy for BI. ROC curve analysis of value of KI for the diagnosis of BI produced AUC of 1(CI: 0.978 to 1.000, p<0.0001). Cut-off value of 33.2 mm for KI was identified for diagnosing BI with 100% accuracy.

CONCLUSION: The distance of tip of the odontoid process from PI line <7.5 mm and value of KI <33.2 mm, both of these parameters can diagnose BI with comparable accuracy to most widely used conventional radiological methods.

KEYWORDS: Basilar Invagination, Palato internal occipital protuberance, Klaus' index, Odontoid process, Chamberlain's line, Diagnosis, Criteria

ABBREVIATIONS: CVJ: Craniovertebral junction, **BI:** Basilar invagination, **FM:** Foramen magnum, **CT:** Computed tomography, **TwL:** Twinning line, **IOP:** Internal occipital protuberance, **KI:** Klaus' Index, **PI:** Palato internal occipital protuberance

INTRODUCTION

The craniovertebral junction (CVJ) is the transitional landmark connecting the head and the vertebral column. It comprises the occiput, atlas, and axis. The CVJ region incorporates numerous osseoligamentous and vital neurovascular structures prone to congenital and acquired malformations (15).

Basilar invagination (BI) is one of the most common CVJ malformations. It is characterized by the protrusion of the odontoid process into the foramen magnum (FM), resulting in the compression of the cervicomedullary junction (14,15,20). Various etiologies contribute to BI, such as hypoplasia of the clivus and condyles of the occipital bone, hypoplasia of the atlas, achondroplasia, atlantooccipital assimilation, and degenerative processes like rheumatoid arthritis, among others (26).

Previously, the diagnosis of BI relied on autopsy findings; however, in 1911, Schullar made a significant breakthrough by establishing the first radiological diagnosis of BI in a living patient (22). Various radiological parameters have since been developed to define BI through linear and angular cra-

Vikrant YADAV : 0009-0000-2980-6479
Nityanand PANDEY : 0000-0002-9594-5992
Anurag SAHU : 0000-0002-7857-4886
Ravi Shankar PRASAD : 0000-0002-4854-9030

niometric measurements, utilizing conventional radiographs, magnetic resonance imaging (MRI), and computed tomography (CT) scans (2,4,8,9,13,24). Linear craniometric methods often employ several anatomical lines for BI diagnosis, including McRae's, Chamberlain's, and McGregor's lines and the Wackenheim clivus baseline (4,8,10,11,27). Other craniometric lines (i.e., Fishgold digastric and bimastoid lines) are less commonly used.

The above mentioned craniometric lines rely on basion and opisthion, which exhibit inherent anatomical variations in the general population concerning their measurements and positions. Associated anomalies of the occipital bones, such as congenital atlantal occipitalization (prevalence rate of 0.08%–2.8%), further pose challenges in accurately delineating these landmarks. Conditions like clival hypoplasia, condylar hypoplasia, achondroplasia, and torticollis also contribute to difficulties in accurately defining the position of basion and opisthion (3,5). Additionally, surgical procedures used for correcting CVJ malformations may involve the removal of parts of the occipital bone, such as FM decompression. Consequently, these craniometric lines become irrelevant for diagnosing BI and establishing comparisons with preoperative measurements in the postoperative period.

To address these challenges, we need landmarks that are readily identifiable radiologically and remain constant in relation to each other during the preoperative and postoperative phases. The following lines, utilized in this study, are examined to determine their efficacy as diagnostic tools in assessing BI.

1. Twinning line (TwL): This is a line connecting the tuberculum sellae and the internal occipital protuberance (IOP) (Figure 1A). Klaus' index (KI), representing the perpendicular distance between the tip of the odontoid process and TwL, is measured (Figure 1B). A lower value of KI serves as an indicator of BI (9,12).
2. Palato–IOP (PI) line: This line connects the posterior part of the hard palate to the IOP (Figure 2A). A perpendicular length between the tip of the odontoid process and the PI line of <9 mm is used as a criterion for diagnosing BI (Figure 2B) (21).

This study aimed to establish the diagnosis of BI based on the values of KI and the perpendicular distance between the tip of the odontoid process and the PI line. Additionally, we aimed to investigate the conventional method of diagnosing BI, which involves assessing the relation of the tip of the odontoid process with Chamberlain's line and measuring the length of the odontoid process above this line.

MATERIAL and METHODS

This retrospective study was conducted in the Department of Neurosurgery at a tertiary care center in northern India between July 2020 and June 2023. Initially, 70 patients who underwent surgery for BI were analyzed. However, 21 were excluded due to the unavailability of appropriate scans to define the required bony landmarks or because they were either younger than 18 or older than 70. Eventually, 49 patients were included in our study. Additionally, we enrolled a control group comprising 120 subjects (age range of 18–70 years) who were screened for spine injuries following a history of head or cervical spine injury, showing no radiological abnormalities on CT scans. Ethical clearance for this study was obtained from the local institutional ethical committee (EC/2023/3094; Dated 30/5/2023.

Figure 1: A) Midsagittal reconstructed images of computed tomography scan of the craniovertebral junction and cervical spinal demonstrating twinning line extending between tuberculum sellae and internal occipital protuberance (white arrow). **B)** Midsagittal reconstructed images of computed tomography scan of the craniovertebral junction and cervical spinal demonstrating measurement of Klaus' index (small arrow) which is extending from tip of odontoid process to twinning line (large arrow).

Figure 2: A) Midsagittal reconstructed images of computed tomography scan of the craniovertebral junction and cervical spinal region demonstrating palato- internal occipital protuberance (PI) line between the tip of posterior end of the hard palate and the internal occipital protuberance (white arrow). **B)** Midsagittal reconstructed images of computed tomography scan of the craniovertebral junction and cervical spine demonstrating measurement of perpendicular distance of the tip of the odontoid process (thin arrow) from palato-internal occipital protuberance line (thick arrow).

CT Imaging Protocol

A 128-slice spiral CT scanner (Discovery Ultra, GE) was employed for the computed tomography scan. The rotator time was 0.5 s/rotation, with parameters set at 120 kVp and 200 mAs. The slice thickness and interval were both 0.625 mm, the field of view measured 240 mm × 240 mm, and the matrix size was 512 × 512. Radiological assessment was conducted in all patients utilizing reconstructed midsagittal images.

Craniometric Analysis

The PI line was delineated, extending from the posterior end of the hard palate to the IOP. Then, the perpendicular distance (mm) between the tip of the odontoid process and the PI line was measured. In cases where the tip of the odontoid process touched or crossed the PI line, this length was considered zero. The TwL was drawn, connecting the tuberculum sellae and the IOP. The KI was calculated by measuring the perpendicular distance (mm) between TwL and the tip of the odontoid process. Chamberlain's line was drawn from the posterior pole of the hard palate to the opisthion, and the length between the tip of the odontoid process above Chamberlain's line was measured (mm).

Statistical Analysis

The data entry was conducted using the Microsoft Excel spreadsheet, and the final analysis was performed using the Statistical Package for Social Sciences (SPSS) software version 25.0 (IBM, Chicago, IL, USA). Categorical variables were presented as numbers and percentages (%). Quantitative data with normal distribution were expressed as mean ± SD, while data with non-normal distribution were presented as median with 25th and 75th percentiles (interquartile range). Normality was assessed using the Kolmogorov–Smirnov test, and non-parametric tests were applied when data were non-normal. The Mann–Whitney test (for two groups) and the Kruskal–Wallis test (for more than two groups) were employed for quantitative variables not normally distributed. Variables with a normal distribution were analyzed using the independent t-test (for two groups) and ANOVA (for more than two groups). The analysis of qualitative variables utilized the chi-square test, and Fisher's exact test was employed if any cell had an expected value of <5. Receiver operating characteristic (ROC) curves were utilized to evaluate the cut-off point, sensitivity, specificity, positive predictive value (PPV), and negative predictive value (NPV) of KI, distance of the tip of the odontoid process from the PI line (mm), and length of the tip of the odontoid process above Chamberlain's line (mm) in predicting BI. Statistical significance was set at a p-value of <0.05. Given the random selection of the control group, there may be potentially significant differences in age and gender between the groups. Therefore, age- and gender-adjusted statistical methods were employed to avoid potential biases in the results.

RESULTS

Demographic Analysis

In this study, we analyzed a cohort of 49 patients who underwent surgery for BI. The mean age of the patients was 34.82 ± 10.52 years (range of 18–70 years), and there was a predominance of males (67.35%, n=33) (Table I). Notably, most patients (93.87%, n=46) were below 40. Additionally, we

examined 120 control subjects (59 males and 61 females) with a mean age of 43.5 ± 14.08 years (range of 18–70 years).

Analysis of BI Based on PI Line

In control subjects, the mean distance of the tip of the odontoid process from the PI line was 12.77 ± 3.03 mm, while in patients with BI, it was 3.39 ± 3.09 mm (Table 2A). The reduction in the mean distance of the tip of the odontoid process from the PI line was statistically significant in patients with BI (p<.0001). Notably, this difference in measurement remained non-significant when comparing various age groups for both the control group (p=0.092) and the patients with BI (p=0.349) (Table 2B). Additionally, gender was not a significant factor for either the control group (p=0.183) or the patients with BI (p=0.639) in relation to this measurement (Table 2C).

Table I: Demographic Characteristics of the Patients with Basilar Invagination

Demographic characteristics	Patients with BI (n=49)
Age (years)	
18-30	15 (30.61%)
31-40	26 (53.06%)
41-50	5 (10.20%)
51-60	1 (2.04%)
61-70	2 (4.08%)
Mean ± SD	34.82 ± 10.52
Gender	
Female	16 (32.65%)
Male	33 (67.35%)

BI: *Basilar Invagination.*

Table IIA: Comparison of the Perpendicular Distance of the Tip of the Odontoid Process from PI line (mm) Between Control Group and Patients with Basilar Invagination

Distance of tip of Odontoid process from PI line (mm)	Mean ± SD
Control group (n=120)	12.77 ± 3.03
Patients with BI (n=49)	3.39 ± 3.09
Total	10.05 ± 5.24
P value	**<.0001***

Independent t test.* ***PI:* *Palato-internal occipital protuberance,* ***BI:*** *Basilar Invagination.*

Analysis of BI on the basis of KI

In the control group, the mean value of KI was 44.57 ± 2.27 mm, while in patients with BI, it was 28.57 ± 1.68 mm (Table 3A). The mean value of KI was significantly reduced in patients with BI (p<.0001). Furthermore, differences in KI measurements were non-significant across various age groups for both the control group (p=0.818) and patients with BI (p=0.064) (Table 3B). In the control group, the mean value of KI was significantly higher for males (p<.0001). However, gender was not associated with the mean value of KI in patients with BI (p=0.603) (Table 3C).

Cut-off Value of the Distance of the Tip of the Odontoid Process from the PI Line and KI for Diagnosing BI

The ROC curve was employed to analyze the distance of the tip of the odontoid process from the PI line for diagnosing BI, resulting in an area under the curve (AUC) of 0.97 (standard error (SE) of 0.0169, confidence interval (CI) of 0.931–0.990, p<0.0001). In ROC analysis, a cut-off point of 7.5 mm was identified for the distance of the tip of the odontoid process from the PI line in this study, where a distance of less than 7.5 mm was indicative of BI. This value exhibited a sensitivity of 89.8% and specificity of 97.5%, with a 93.6% PPV for diagnosing BI (Table IV, Figure 3).

The ROC curve analysis of KI for diagnosing BI revealed an AUC of 1 (CI of 0.978–1.000, p<0.0001). In this study, a determined cut-off value of 33.2 mm for KI in ROC analysis indicated that a KI value below 33.2 mm was diagnostic of BI. This specific value demonstrated 100% specificity and sensitivity and a 100% PPV for diagnosing BI (Table V, Figure 4).

Table IIB: Association of Distance of the Tip of the Odontoid Process from PI Line (mm) with Age Group in the Control Group and the Patients with Basilar Invagination

Age group	Distance if tip of Odontoid process from PI line in control group (Mean ± SD) (in mm)	Distance of tip of Odontoid process from PI line in patients of BI (Mean ± SD) (in mm)
18-30	13.36 ± 2.64 (n=21)	3.16 ± 2.8(n=15)
31-40	12.23 ± 3.26 (n=37)	3.92 ± 3.47 (n=26)
41-50	11.92 ± 2.88 (n=20)	0.84 ± 1.15 (n=5)
51-60	13.95 ± 3.03 (n=27)	3.3 ± 0 (n=1)
61-70	12.31 ± 2.72 (n=15)	4.5 ± 0 (n=2)
Total	12.77 ± 3.03 (n=120)	3.39 ± 3.09 (n=49)
P value	0.092*	0.349*

Anova test.* ***PI:* *Palato-internal occipital protuberance,* ***BI:*** *Basilar Invagination.*

Table IIC: Association of Distance of the Tip of the Odontoid Process from PI Line (mm) with Gender in the Control Group and the Patients with Basilar Invagination.

Gender	Distance of tip of Odontoid process from PI line in control group (mm) (Mean ± SD)	Distance of tip of Odontoid process from PI line in patients of BI (mm) (Mean ± SD)
Female	12.41 ± 2.68 (n=61)	3.69 ± 3.57 (n=16)
Male	13.15 ± 3.34 (n=59)	3.24 ± 2.88 (n=33)
Total	12.77 ± 3.03 (n=120)	3.39 ± 3.09
P value	0.183*	0.639*

Independent t test.* ***PI:* *Palato-internal occipital protuberance,* ***BI:*** *Basilar Invagination.*

Table IIIA: Comparison of Klaus' Index (mm) Between the Control Group and Patients with Basilar Invagination

Klaus ' index (mm)	Mean ± SD
Control group (n=120)	44.57 ± 2.27
Patients with BI (n=49)	28.57 ± 1.68
Total	39.93 ± 7.58
P value	**<.0001***

Independent t test.* ***BI:* *Basilar invagination.*

Table IIIB: Association of Klaus' index (mm) with Age Group in the Control Group and the Patients with Basilar Invagination

Age group	Klaus' index in control group (mm) (Mean ± SD)	Klaus' index in patients with BI (mm) (Mean ± SD)
18-30	44.77 ± 2.9 (n=21)	27.91 ± 1.14 (n=15)
31-40	44.32 ± 1.79 (n=37)	28.67 ± 1.8 (n=26)
41-50	44.49 ± 1.86 (n=20)	28.6 ± 1.7 (n=5)
51-60	44.5 ± 2.68 (n=27)	30.2 ± 0 (n=1)
61-70	45.13 ± 2.2 (n=15)	31.3 ± 0 (n=2)
Total	44.57 ± 2.27 (n=120)	28.57 ± 1.68 (n=49)
P value	0.818*	0.064*

*******Anova test,* ***BI:*** *Basilar invagination.*

Table IIIC : Association of Klaus' index (mm) with Gender in the Control Group and the Patients with Basilar Invagination

Gender	Klaus' index in control group (mm) (Mean ± SD)	Klaus' index in patients with BI (mm) (Mean ± SD)
Female	43.63 ± 2.05 (n=61)	28.39 ± 1.59 (n=16)
Male	45.54 ± 2.08 (n=59)	28.66 ± 1.74 (n=33)
Total	44.57 ± 2.27 (n=120)	28.57 ± 1.68
P value	**<.0001***	0.603*

Independent t test,* ***BI:* *Basilar Invagination.*

Table IV: Receiver Operating Characteristic Curve Analysis of Distance of the Tip of Odontoid Process from Palato- Internal Occipital Protuberance (PI) Line (mm) for Predicting Basilar Invagination

Variables	Distance of tip of odontoid process from PI line (mm)
Area under the ROC curve (AUC)	0.97
Standard Error	0.0169
95% Confidence interval	0.931 to 0.990
P value	**<0.0001**
Cut off	**≤7.5 mm**
Sensitivity (95% CI)	89.8% (77.8 - 96.6%)
Specificity (95% CI)	97.5% (92.9 - 99.5%)
PPV (95% CI)	93.6% (82.5 - 98.7%)
NPV (95% CI)	95.9% (90.7 - 98.7%)
Diagnostic accuracy	95.27%

PI: *Palato internal occipital protuberance,* ***ROC:*** *Receiver operating characteristic,* ***AUC:*** *Area under curve,* ***CI:*** *Confidence Interval,* ***PPV:*** *Positive predictive value,* ***NPV:*** *Negative predictive value.*

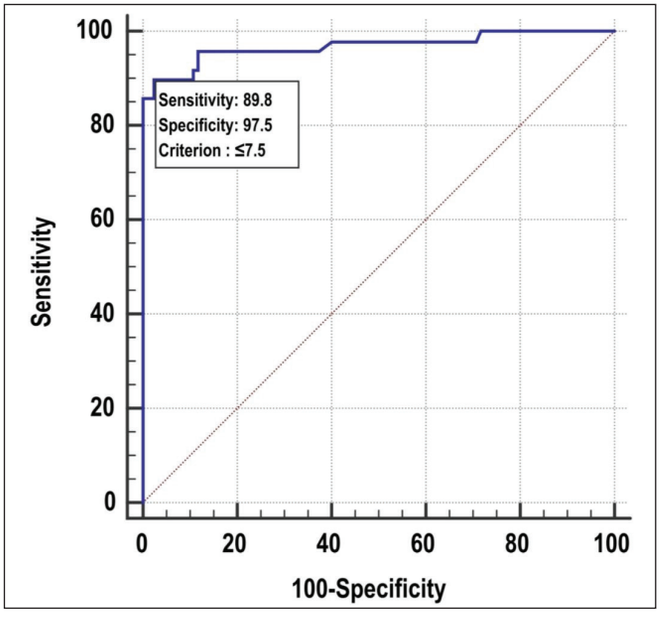

Figure 3: Receiver operating characteristic curve of the perpendicular distance of the odontoid process from palato internal occipital protuberance (PI) line (mm) for predicting BI (AUC-0.97, CI-0.931 to 0.990, p<0.0001, Cut-off value of the distance of the tip of the odontoid process from PI line for the diagnosis of BI is equal or less than 7.5 mm). **BI:** Basilar Invagination, **AU:** Area under curve, **CI:** Confidence Interval.

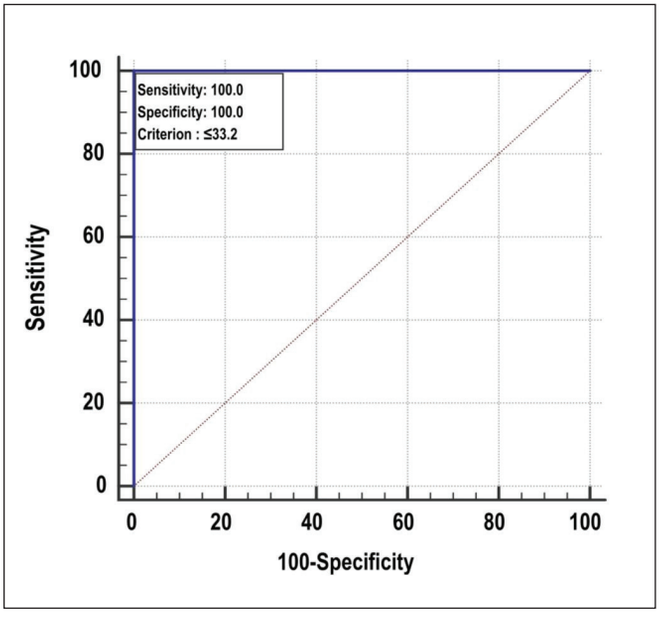

Figure 4: Receiver operating characteristic curve of measurement of Klaus' index for predicting the diagnosis of BI (AUC-1,CI-0.978 to 1, p<0.0001,Cutoff value of measurement of Klaus' index for diagnosing BI is equal or less than 33.2 mm). **BI:** Basilar Invagination, **AUC:** Area under curve, **CI:** Confidence Interval.

Analysis of the Length of the Odontoid Process Above Chamberlain's Line for Diagnosing BI

The median length of the odontoid process above Chamberlain's line was 1.3 (0.3–2.3) mm in the control group and 13.3 (10.3–15.3) mm in patients with BI (Table 6A). This length was significantly higher in patients with BI (p<.0001). ROC analysis of the length of the odontoid process above Chamberlain's line yielded an AUC of 1 (CI of 0.978–1.0, p<0.0001). In our study, a cut-off of 5.3 mm was identified in ROC analysis for the length of the odontoid process above Chamberlain's line, indicating that a length above 5.3 mm was diagnostic of BI. This value demonstrated 100% specificity and sensitivity and a 100% PPV for diagnosing BI (Table 6B, Figure 5).

Table V: Receiver Operating Characteristic Curve of Klaus' Index (mm) for Predicting Basilar Invagination

Variables	Value of Klaus' index (mm)
Area under the ROC curve (AUC)	1
Standard Error	0
95% Confidence interval	0.978 to 1.000
P value	**<0.0001**
Cut off	**≤33.2**
Sensitivity (95% CI)	100% (92.7 - 100.0%)
Specificity (95% CI)	100% (97.0 - 100.0%)
PPV (95% CI)	100% (92.7 - 100.0%)
NPV (95% CI)	100% (97.0 - 100.0%)
Diagnostic accuracy	100.00%

ROC: *Receiver operating characteristic,* ***AUC:*** *Area under curve,* ***CI:*** *Confidence Interval,* ***PPV:*** *Positive predictive value,* ***NPV:*** *Negative predictive value.*

Table VIA: Comparison of Length of the Odontoid Process Above Chamberlain's Line (mm) in Between the Control Group and the Patients with Basilar Invagination

Length of odontoid above Chamberlain's line (mm)	Median (25^{th}-75^{th} percentile)
Control group (n=120)	1.3 (0.3-2.3)
Patients with BI (n=49)	13.3 (10.3-15.3
Total	2.2 (0.8-9.3)
P value	<.0001

DISCUSSION

BI is one of the most prevalent malformations in the CVJ region, frequently affecting the adult population (6,14,28). Chamberlain's line is one of the extensively used linear craniometric parameters in the radiological assessment of BI (6,7). The normal range for the length of the tip of the odontoid

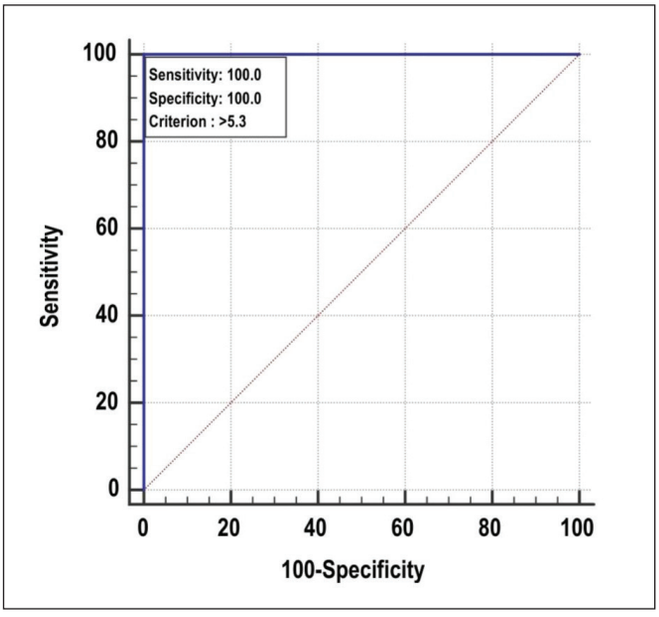

Figure 5: Receiver operating characteristic curve of measurement of the length of the odontoid process above Chamberlain's line to diagnose BI (AUC-1, CI- 0.978 to 1, p<0.0001, Cut-off value of the measurement of the length of the odontoid process above Chamberlain's line for diagnosing BI is more than 5.3 mm). **BI:** Basilar invagination, **AUC:** Area under curve, **CI:** Confidence interval.

Table VIB: Receiver Operating Characteristic Curve Analysis of Length of the Odontoid Process Above Chamberlain's line (mm) for Predicting Basilar Invagination

Variables	Length of odontoid process above Chamberlain's line (mm)
Area under the ROC curve (AUC)	1
Standard Error	0
95% Confidence interval	0.978 to 1.000
P value	**<0.0001**
Cut off	**>5.3**
Sensitivity (95% CI)	100% (92.7 - 100.0%)
Specificity (95% CI)	100% (97.0 - 100.0%)
PPV (95% CI)	100% (92.7 - 100.0%)
NPV (95% CI)	100% (97.0 - 100.0%)
Diagnostic accuracy	100.00%

ROC: *Receiver operating characteristic,* **AUC:** *Area under curve,* ***CI:*** *Confidence Interval,* ***PPV:*** *Positive predictive value,* ***NPV:*** *Negative predictive value.*

process above Chamberlain's line can vary across different studies (24,25,27). In this study, a length above 5.3 mm of the odontoid process above Chamberlain's line demonstrated excellent diagnostic accuracy for BI. This finding aligns with several other studies (1,4,18,19,23,27).

Pitfalls in the Measurement of the Length of the Odontoid Process Above Chamberlain's Line for Diagnosing BI

The measurement of Chamberlain's line involves identifying basion and opisthion. However, determining the positions of these landmarks can be challenging in the presence of CVJ malformations such as occipitalization of atlas, condylar and clival hypoplasia, asymmetrical facet joints, and achondroplasia (18,23,27). This difficulty may arise owing to the uneven level of basion and opisthion or the overlap of the facet joint with basion and opisthion. Positional changes of the neck can also influence variability in the position of basion and opisthion during imaging. Another significant drawback of these conventional parameters is that, following surgical procedures like FM decompression, these measurements significantly change compared to their preoperative values (3,5,21).

Reasons for Using the Distance of the Tip of the Odontoid Process from the PI Line

The distance between the tip of the odontoid process and the PI line is a valuable tool for establishing BI, as evidenced by this study. A distance less than 7.5 mm between the tip of the odontoid process and the PI line was significantly associated with the presence of BI. The bony landmarks involved in this measurement can be easily identified on conventional radiographs and CT imaging, and they remain constant irrespective of the type of CVJ malformations, positional changes, or surgical procedures performed. Sardhara et al. previously demonstrated that a distance of the odontoid tip to the PI line of <9 mm was a highly applicable criterion for diagnosing BI. They noted a 15%–20% variability in clival length and occipital length, leading to significant changes in the positions of basion and opisthion (21).

Reasons for Using KI

The measurement of KI involves key bony landmarks, including the tuberculum sellae, IOP, and the tip of the odontoid process. The relative constancy and easy identification of tuberculum sellae and IOP on conventional radiographs and CT scans make them robust markers, unaffected by various CVJ malformations associated with BI or surgical procedures. Despite previous exploration in the context of Chiari malformation, literature regarding the utility of KI in diagnosing BI remains unsatisfactory. The usual range of KI varies from 30 to 41 mm across different studies (16,17). In this study, values of KI below 33.2 mm were significantly associated with BI, demonstrating 100% diagnostic accuracy.

While Chamberlain's line has conventionally been used for BI diagnosis, the anatomical variability of landmarks poses challenges in its clinical application. To address these challenges, we propose two craniometric parameters based on fixed bony landmarks that are readily identifiable through conventional radiological methods and highly diagnostic for BI.

Limitations

The retrospective nature of the study and its limited sample size introduce potential biases. Another limitation is the absence of an assessment of interobserver variability in our study. Nevertheless, this investigation serves as a preliminary step, laying the groundwork for future prospective studies with a larger sample size.

CONCLUSION

Both the distance of the tip of the odontoid process from the PI line (< 7.5 mm) and a value of KI (<33.2 mm) serve as highly diagnostic craniometric parameters for BI. These parameters demonstrate a diagnostic accuracy comparable to the most widely used lines in conventional radiological methods, regardless of associated CVJ malformations or surgical procedures of the posterior fossa, such as FM decompression.

AUTHORSHIP CONTRIBUTION

Study conception and design: NP, AS

Data collection: VY, NP

Analysis and interpretation of results: VY, RSP

Draft manuscript preparation: VY, AS

Critical revision of the article: NP, RSP

Other (study supervision, fundings, materials, etc...): VY, NP, AS, RSP

All authors (VY, NP, AS, RSP) reviewed the results and approved the final version of the manuscript.

REFERENCES

1. Baysal B, Eser MB, Sorkun M: Radiological approach to basilar invagination type B: Reliability and accuracy. J Neuroradiol 49:33-40, 2022. https://doi.org/10.1016/j.neurad.2020.08.005
2. Botelho RV, Ferreira ED: Angular craniometry in craniocervical junction malformation. Neurosurg Rev 36:603-610; discussion 610, 2013. https://doi.org/10.1007/s10143-013-0471-0
3. Burwood RJ, Watt I: Assimilation of the atlas and basilar impression: A review of 1,500 skull and cervical spine radiographs. Clin Radiol 25:327-333, 1974. https://doi.org/10.1016/S0009-9260(74)80159-5
4. Chamberlain WE: Basilar impression (Platybasia): A bizarre developmental anomaly of the occipital bone and upper cervical spine with striking and misleading neurologic manifestations. Yale J Biol Med 11:487-496, 1939
5. Chevrel JP: Occipitalization of the atlas. Arch Anat Pathol 13:104-108, 1965. (In French)
6. Donnally III CJ, Munakomi S, Varacallo M: Basilar invagination. [Updated 2023 Feb 12]. In: StatPearls [Internet]
7. Ferreira JA, Botelho RV: The odontoid process invagination in normal subjects, Chiari malformation and Basilar invagination patients: Pathophysiologic correlations with angular craniometry. Surg Neurol Int 6:118, 2015. https://doi.org/10.4103/2152-7806.160322
8. Goel A: Basilar invagination, Chiari malformation, syringomyelia: A review. Neurol India 57:235-246, 2009. https://doi.org/10.4103/0028-3886.53260

9. Goel A, Bhatjiwale M, Desai K: Basilar invagination: A study based on 190 surgically treated patients. J Neurosurg 88:962-968, 1998. https://doi.org/10.3171/jns.1998.88.6.0962
10. Jain N, Verma R, Garga UC, Baruah BP, Jain SK, Bhaskar SN: CT and MR imaging of odontoid abnormalities: A pictorial review. Indian J Radiol Imaging 26:108-119, 2016. Doi: 10.4103/0971-3026.178358. https://doi.org/10.4103/0971-3026.178358
11. Karagoz F, Izgi N, Kapijcijoglu Sencer S: Morphometric measurements of the cranium in patients with Chiari type I malformation and comparison with the normal population. Acta Neurochir (Wien) 144:165-171; discussion 171, 2002. https://doi.org/10.1007/s007010200020
12. Klaus E: Roentgen diagnosis of platybasia & basilar impression; additional experience with a new method of examination. Fortschr Geb Rontgenstr Nuklearmed 86:460-469, 1957. (In German) https://doi.org/10.1055/s-0029-1213168
13. Koenigsberg RA, Vakil N, Hong TA, Htaik T, Faerber E, Maiorano T, Dua M, Faro S, Gonzales C: Evaluation of platybasia with MR imaging. AJNR Am J Neuroradiol 26:89-92, 2005
14. Lan S, Xu J, Wu Z, Xia H, Ma X, Zhang K, Ai F, Wang J, Yin Q, Yi H, Duan M: Atlantoaxial joint distraction for the treatment of basilar invagination: Clinical outcomes and radiographic evaluation. World Neurosurg 111:e135-e141, 2018. https://doi.org/10.1016/j.wneu.2017.12.013
15. Lopez AJ, Scheer JK, Leibl KE, Smith ZA, Dlouhy BJ, Dahdaleh NS: Anatomy and biomechanics of the craniovertebral junction. Neurosurg Focus 38:E2, 2015. https://doi.org/10.3171/2015.1.FOCUS14807
16. Madeddu R, Cecchini A, Mazzarello V, Sotgiu MA, Farace C, Bandiera P: Agenesis of the posterior arch of the atlas and complex alterations of the craniovertebral junction: A case report. Radiol Case Rep 14:1151-1155, 2019. https://doi.org/10.1016/j.radcr.2019.05.033
17. Maheshwari S, Bhat V, Kumar Bn K: Imaging of normal and abnormal cranio-vertebral junction - A pictorial review. HSOA J Brain Neurosci Res 5:018, 2021
18. McRAE DL: Bony abnormalities in the region of the foramen magnum: Correlation of the anatomic and neurologic findings. Acta Radiol 40:335-543, 1953. https://doi.org/10.3109/00016925309176595
19. Nascimento JJC, Neto EJS, Mello-Junior CF, Valença MM, Araújo-Neto SA, Diniz PRB: Diagnostic accuracy of classical radiological measurements for basilar invagination of type B at MRI. Eur Spine J 28:345-352, 2019. https://doi.org/10.1007/s00586-018-5841-4
20. Ottenhausen M, Alalade AF, Rumalla K, Nair P, Baaj A, Hartl R, Kacker A, Greenfield JP, Anand VK, Schwartz TH: Quality of life after combined endonasal endoscopic odontoidectomy and posterior suboccipital decompression and fusion. World Neurosurg 116:e571-e576, 2018. https://doi.org/10.1016/j.wneu.2018.05.041
21. Sardhara J, Behari S, Singh S, Srivastava AK, Chauhan G, Lal H, Das KK, Bhaisora KS, Mehrotra A, Mishra P, Jaiswal AK: A universal craniometric index for establishing the diagnosis of basilar invagination. Neurospine 18:206-216, 2021. https://doi.org/10.14245/ns.2040608.304
22. Schuller A: Zur Roentgendiagnose der basilaren impression des schädels. Wien Med Wochenschr 61:2594, 1911
23. Serindere G, Gunduz K, Avsever H: Morphological measurement and anatomical variations of the clivus using computed tomography. J Neurol Surg B Skull Base 83 Suppl 2:e75-e82, 2021. https://doi.org/10.1055/s-0040-1722712
24. Shah A, Serchi E: Management of basilar invagination: A historical perspective. J Craniovertebr Junction Spine 7:96-100. https://doi.org/10.4103/0974-8237.181856
25. Silva ATPB, Silva LTPB, Vieira AENR, de Melo CIE, do Nascimento JJC, de Mello Júnior CF, Vasconcelos SC, de Araújo-Neto SA: Craniometric parameters for the evaluation of platybasia and basilar invagination on magnetic resonance imaging: A reproducibility study. Radiol Bras 53:314-319, 2020. https://doi.org/10.1590/0100-3984.2019.0068
26. Smith JS, Shaffrey CI, Abel MF, Menezes AH: Basilar invagination. Neurosurgery 66 Suppl 3:39-47, 2010. https://doi.org/10.1227/01.NEU.0000365770.10690.6F
27. Smoker WR: Craniovertebral junction: Normal anatomy, craniometry, and congenital anomalies. Radiographics 14:255-277, 1994. https://doi.org/10.1148/radiographics.14.2.8190952
28. Wang X, Ma L, Liu Z, Chen Z, Wu H, Jian F: Reconsideration of the transoral odontoidectomy in complex craniovertebral junction patients with irreducible anterior compression. Chin Neurosurg J 6:33, 2020. https://doi.org/10.1186/s41016-020-00210-4